Am J Physiol Heart Circ Physiol 283: H1282–H1291, 2002.
First published June 13, 2002; 10.1152/ajpheart.00117.2002.

Role of glycocalyx in leukocyte-endothelial cell adhesion

A. W. MULIVOR AND H. H. LIPOWSKY
Department of Bioengineering, Pennsylvania State University, University Park, Pennsylvania 16802

Received 25 February 2002; accepted in final form 5 June 2002

Mulivor, A. W., and H. H. Lipowsky. Role of glycocalyx in leukocyte-endothelial cell adhesion. *Am J Physiol Heart Circ Physiol* 283: H1282–H1291, 2002. First published June 13, 2002; 10.1152/ajpheart.00117.2002.—The binding of fluorescently labeled microspheres (FLMs, 0.1-μm diameter) coated with antibody (1a29) to ICAM-1 was studied in postcapillary venules during topical application of the chemoattractant *N*-formylmethionyl-leucyl-phenylalanine (fMLP). FLM adhesion to endothelial cells (ECs) increased dramatically from 50 to 150 spheres per 100-μm length of venule after superfusion of the mesentery with fMLP and equaled or exceeded levels of leukocyte (WBC) adhesion. Removal of the EC glycocalyx by micropipette infusion of the venule with heparinase increased FLM-EC adhesion to levels attained with fMLP. Subsequent application of fMLP did not increase FLM adhesion further, suggesting that the FLMs saturated all ICAM-1 binding sites. Perfusion with heparinase after suffusion with fMLP significantly increased FLM-EC adhesion above levels attained with fMLP. However, WBC adhesion fell because of possible removal of selectins necessary to maintain WBC rolling at the wall. It is concluded that the glycocalyx serves as a barrier to adhesion and that its shedding during natural activation of ECs may be an essential part of the inflammatory response.

endothelium; heparinase; *N*-formylmethionyl-leucyl-phenylalanine

MICROVASCULAR ENTRAPMENT and diapedesis of leukocytes (WBCs) in the inflammatory process revolves around a well-defined sequence of events that encompass the radial migration (margination) of WBCs toward the endothelium (26), selectin-mediated rolling along the venular wall (24), and integrin-mediated firm adhesion of WBCs to the endothelium (10). Direct observations by intravital microscopy of WBC rolling along endothelial cells (ECs) and adhesion in postcapillary venules have provided much quantitative data on the strength of WBC-EC bonds and the receptor-ligand pairs involved. A common approach to these studies has been to topically apply various stimuli to promote WBC-EC interaction and to measure the rolling velocity of WBCs or the number of cells firmly adhered and to quantitate hydrodynamic forces acting to dislodge WBCs from the EC. For example, the pioneering studies of Atherton and Born (3) used exposure of the mesenteric tissue to mechanical handling and inflammatory agents (e.g., caseine and histamine) and recorded WBC rolling velocity and numbers of firmly adhered cells to quantitate the extent of WBC-EC adhesion. Subsequent studies examined rolling and adhered WBCs in exteriorized microvascular preparations to elucidate the role of various chemoattractants and cytokines in stimulating adhesion, such as leukotriene B_4 (2), platelet-activating factor (4), tumor necrosis factor (TNF)-α (15), and formyl peptide *N*-formylmethionyl-leucyl-phenylalanine (fMLP) (11, 22), to name a few. Most in vivo studies of this type have recognized the potential of these agents to activate both the WBC and the EC; however, attempts to systematically activate these cells individually have not been performed. To address this void in the literature, the present study was undertaken to examine the adhesion of inert polystyrene microspheres coated with MAb to adhesion molecules on the endothelium, principally ICAM-1 (CD 54) during topical application of fMLP to intestinal mesentery.

The initial objective of the present study was to compare the rates of sequestration of systemically infused MAb-coated spheres, 0.1 μm in diameter, to those of WBCs, to thus test the hypothesis that WBC-EC adhesion is dominated by the process of WBC activation by suffusion of the mesentery with fMLP. To that end, studies were first performed to determine the appropriate concentration of microspheres to minimize concentration effects. Spheres were subsequently infused at a steady rate into the femoral vein, and their adhesion to the walls of postcapillary venules was evaluated under resting (control) conditions and in response to superfusion with fMLP. On finding that the transient increase in sphere adhesion in response to fMLP was similar in magnitude to that of WBC-EC adhesion and that the spatial distribution of adherent spheres was limited to focal adhesion sites because of their apparently restricted access to the EC, we conducted additional studies to elucidate the role of the endothelial glycocalyx in modulating adhesion events of spheres and WBCs. For this purpose, individual postcapillary venules were cannulated with micropipettes, perfused with heparinase to remove the glycocalyx, and then subjected to a steady influx of spheres from the pipette or WBCs from proximal microvessels.

Address for reprint requests and other correspondence: H. H. Lipowsky, Dept. of Bioengineering, Penn State Univ., 233 Hallowell Bldg, University Park, PA 16802 (E-mail: HHLBIO@engr.psu.edu).

The costs of publication of this article were defrayed in part by the payment of page charges. The article must therefore be hereby marked "*advertisement*" in accordance with 18 U.S.C. Section 1734 solely to indicate this fact.

METHODS

Animal Preparation and Intravital Microscopy

Male Sprague-Dawley rats weighing 350–450 g were anesthetized with pentobarbital sodium (45 mg/kg ip), tracheostomized, and allowed to breathe spontaneously. The right internal jugular vein was cannulated with polyethylene (PE-50) tubing to enable administration of supplemental doses of anesthetic as required to maintain a surgical plane of anesthesia. The left carotid artery was cannulated with PE-90 tubing and connected to a strain gauge-type pressure transducer to monitor arterial blood pressure. To facilitate systemic infusion of fluorescently labeled microspheres (FLMs) the right femoral vein was cannulated with PE-10 tubing and connected to an infusion syringe pump (Harvard Apparatus, Holliston, MA). The systemic Hct (Hct_{sys}), WBC count, and circulating FLM concentration ($[FLM]_{circ}$) were measured by withdrawing 0.25 ml of blood through the carotid catheter. Leukocyte counts were obtained with a Coulter counter (model ZM; Beckman-Coulter, Miami, FL). For all animals studied, the WBC count averaged 7,682 ± 2,369 (SD) cells/μl and Hct_{sys} averaged 46.7 ± 3.4 (SD)%. FLM counts were obtained by using a hemocytometer while viewing under a fluorescence microscope.

The intestinal mesentery was exteriorized through a midline abdominal incision and placed on a glass pedestal to facilitate viewing under either brightfield microscopy by transillumination or incident illumination with a Ploeme-type fluorescence illuminator with fluorescein excitation and emission filters. The tissue was suffused with HEPES-buffered Ringer solution (pH = 7.4) at a temperature of 37.0°C. Solutions of fMLP (10^{-7} M; Sigma, St. Louis, MO) were prepared in HEPES-buffered Ringer solution (pH 7.4) for irrigation of the tissue.

Mesenteric postcapillary venules ranging in width from 25 to 50 μm were viewed with either a Leitz UM ×20/0.33 numerical aperture (NA) (true magnification ×13/0.22 NA) or a Zeiss water-immersion ×40/0.75 NA objective. The image was projected onto a low-light-level silicon-intensified target camera (model 66; Dage-MTI, Michigan City, IN), for an effective width of the video field equal to 310 or 100 μm, respectively.

Fluorescent Microsphere Preparation

Fluorescent (yellow-green) carboxylate-modified polystyrene microspheres, 0.1 μm in diameter (Fluospheres; Molecular Probes, Eugene, OR), were labeled with 1a29 (IgG_1) (26) MAb to rat ICAM-1 (a generous gift of Dr. Donald Anderson, Pharmacia and Upjohn Laboratories, Kalamazoo, MI). A nonreactive control MAb, Marg1–2 (IgG_1) mouse anti-rat, was obtained from Zymed Laboratories (San Francisco, CA) for determining binding specificity.

FLMs were prepared by first binding protein G (PG) as a functional spacer between the microsphere and the 1a29 MAb. PG was chosen because of its superior binding properties to mouse IgG_1 antibodies compared with protein A and protein AG (1). This procedure entailed a two-step process. The first stage of the binding protocol involved binding the amine group on the PG to a carboxyl group on the FLM with the carbodiimide reaction (6). The carbodiimide reaction requires activation of the amine group on the PG at pH 8.5 and activation of the carboxyl group of the FLM at pH 4.5. The carbodiimide solution of 1-ethyl-3-(3-dimethylaminopropyl) carbodiimide facilitated the reaction between the two activated functional groups.

The second stage of the binding protocol involved binding the Fc region of the 1a29 MAb to the free carboxyl end of the PG, leaving the functional Fab group available for binding to ICAM-1. The Fc region of the 1a29 contains several carbohydrate residues (13) that are ideal to bind the PG under mildly acidic conditions of pH = 4–7. SDS-PAGE was performed to quantitate the extent of PG and 1a29 binding. The final supernatant of the sphere suspension revealed an absence of PG and 1a29 (<1 μg/ml), and calculations suggested a final binding ratio of 88 1a29 molecules/FLM.

Micropipette Preparation and Infusion Protocol

Glass capillary tubes with a 1-mm outer diameter and a 0.75-mm inner diameter (TW100F-6; World Precision Instruments, Sarasota, FL) were drawn into micropipettes with a vertical pipette puller (model 700-C; David Kopf Instruments, Tujunga, CA). The tips of the micropipettes were double-beveled at a 30° angle with a micropipette beveler (model BV-10; Sutter Instrument, Novato, CA). The luminal diameters at the tip of the micropipette (6–9 μm) were measured by video microscopy (image-shearing monitor; IPM, San Diego, CA) calibrated against a stage micrometer. Micropipettes were filled with, and stored in, normal saline. Solutions with microspheres of desired concentrations were back loaded into the micropipette with a 34-gauge syringe.

Micropipettes were held in a micromanipulator, and the back end of each pipette was connected to a pressure reservoir monitored with a manometer. A set of calibration curves was established to express the volumetric effluent from the pipette tip as a function of tip luminal diameter and back pressure. The volume flow rate emanating from the tip was measured for a specified back pressure by recording the diameter of the spherical bubble formed in air, while being viewed under the microscope, and calculating the effluent volume as a function of time.

Sphere-laden micropipettes were held in a micromanipulator with its back end connected to the pressure reservoir. After intubation of postcapillary venules, the pipette back pressure was adjusted to deliver a flow rate that matched (within 5%) the volumetric flow rate measured within the venule, as obtained from measurements of red blood cell velocity (V_{RBC}) before the intubation. All solutions were infused continuously as needed.

Red Blood Cell Velocity and Volumetric Flow

The center line V_{RBC} in arterioles and venules was measured with the two-slit photometric technique (31) using a self-tracking correlator (27). The mean velocity of blood (V_{mean}) was calculated from the relationship $V_{mean} = V_{RBC}/1.6$ (16). The vessel diameter (D) was measured with video image shearing. Volumetric flow rate of blood in the venules (Q) was calculated as the product of V_{mean} and the cross-sectional area, $\pi D^2/4$, assuming a circular cross section.

Experimental Protocols

Two separate protocols were employed. The first protocol entailed continuous infusion of 1a29-FLMs into the femoral vein at a concentration ranging from 0.5 to 5.7 × 10^8 spheres·ml^{-1}·kg^{-1} at a rate of 0.02 ml/min to achieve a desired systemic concentration. The second protocol entailed intubating venules with micropipettes filled with either FLMs at the desired concentration or heparinase (1 U/ml in normal saline; Sigma) to strip off the venular glycocalyx. In the latter case, FLM and WBC adhesion were observed under control conditions and in response to superfusion of the

mesentery with fMLP before and after removal of the glycocalyx.

For each protocol, the mesenteric tissue was allowed to stabilize for 30 min before data acquisition. Unbranched postcapillary venules, 25–45 μm in diameter, with lengths of at least 150 μm were chosen for analysis. Micropipettes were inserted into proximal side branches to permit perfusion of the venule with FLMs, heparinase, or blood from proximal microvessels.

Measurements

WBC and FLM adhesion. The numbers of WBCs and FLMs firmly adhered were measured by frame-by-frame analysis of video recordings and normalized in terms of the number adhering per 100 μm of venule length. Adhered WBCs and FLMs were judged to be firmly adhered if they remained stationary for at least 5 s. All FLMs and WBCs were counted by focusing the microscope objective above and below the diametral plane.

WBC rolling flux and adhesion. The flux of WBCs rolling along the venular endothelium was measured by frame-by-frame analysis of video recordings and was normalized with respect to the potentially maximal flux of WBCs carried within the venular lumen by computing the fractional flux, F_{WBC}. F_{WBC} was calculated with established techniques (8) as the ratio of rolling flux (cells/min) to the product of microvessel bulk flow (Q) and systemic leukocrit (Lct) divided by WBC mean cell volume (mcv): F_{WBC} = (rolling flux × mcv/Q × Lct).

RESULTS

Examination of Microsphere Specificity

Initial experiments were performed to test the specificity of the binding of the 1a29-FLM to the vascular endothelium. FLMs representing different stages of the antibody labeling protocol were infused systemically to test their respective specificity for binding to the endothelium. Unaltered carboxylated spheres were dialyzed against PBS and infused into the femoral vein. These spheres immediately adhered to themselves and to the vascular endothelium, causing vascular stasis. Protein G-coated FLMs were infused systemically at concentrations ranging from 1.1 to 8.5 × 10^6/mm^3. These spheres adhered to the endothelium at a level of 1.2 ± 0.7 (control conditions) to 2.5 ± 0.46 (fMLP superfusion) spheres per 100 μm of venule length. FLMs were prepared with a control antibody (Marg1–2) with the same isotype (IgG_1) as the anti-ICAM-1 1a29, but not the specificity. The Marg1–2 antibody was coated onto the FLMs with the same protocol used for the 1a29 antibody. The results of the Marg1–2 FLM adhesion revealed maximum values of 3.2 ± 0.52 (under control conditions) and 3.49 ± 0.42 spheres/100 μm (with fMLP superfusion). In all cases the adhesion of the control FLMs was significantly less than the adhesion of the 1a29-FLMs, which typically ranged from 20 (control) to 150 (fMLP stimulated) spheres/100 μm.

To determine whether the process of linking the 1a29 antibody to the microspheres affected the specificity of the sphere-bound 1a29 for ICAM-1, individual venules (n = 10) were intubated with micropipettes and perfused with soluble 1a29 (1 mg/ml) in PBS for 10 min. These venules were then perfused with 1a29-FLMs (10^7 spheres/mm^3) for 20 min, under conditions of tissue superfusion with either Ringer solution (control) or fMLP. After perfusion with soluble 1a29, adhesion levels equaled 2.41 ± 2.0 (SD) spheres/100 μm and 4.0 ± 1.5 spheres/100 μm, respectively. In similar experiments (n = 10) without perfusion with soluble 1a29, a significant level of adhesion was found to equal 67.3 ± 4.3 spheres/100 μm with Ringer superfusion, and 163.5 ± 4.5 spheres/100 μm after fMLP superfusion ($P < 0.001$). Thus, although there was a significant level ($P < 0.001$) of nonspecific adhesion, it amounted to <4% of that observed without perfusion with soluble 1a29.

Systemic FLM Infusion

To determine the optimum circulating concentration of 1a29-FLMs, different concentrations ($[FLM]_{circ}$) were infused via the femoral vein (syringe pump) to achieve concentrations of 1.11, 2.43, 4.32, 8.46, and 10.87 × 10^6/mm^3. Representative images of a postcapillary venule (D = 36.2 μm) with $[FLM]_{circ}$ = 4.32 × 10^6/mm^3 are presented in Fig. 1 under control conditions and after 42-min suffusion with fMLP. The brightfield images (Fig. 1, *A* and *C*) reveal the expected dramatic rise in WBC adhesion from ~1 to 20 WBCs/100 μm. The fluorescence images (Fig. 1, *B* and *D*) reveal a rise in FLM adhesion from 12 to 133 spheres/100 μm in response to the fMLP. The distribution of FLMs was easily discernible under fluorescence microscopy despite the occurrence of blurring of out-of-focus spheres. By focusing the microscope up and down, the presence of adhered spheres could be readily evaluated. As in the case of the WBCs, the distribution of adherent FLMs appeared patchy and confined to discrete regions along the length of the vessel. However, the majority of FLMs appeared to be distributed without interfering with WBC adhesion, and there does not appear to be a shortage of binding sites for the spheres caused by adherent WBCs.

The transient process of WBC and FLM adhesion to the endothelium is illustrated in Fig. 2. Infusion of FLMs into the femoral vein (syringe pump) were begun at time zero to achieve a steady state $[FLM]_{circ}$ equal to 4.2 × 10^6/mm^3. The concentration of adherent FLMs reached a steady level of 14 spheres/100 μm within 10 min and remained constant until fMLP superfusion of the tissue was begun at 20 min after the start of infusion. During the next 20 min, FLMs rose to a maximal level of 130 spheres/100 μm. WBCs achieved maximal adhesion within 10 min of onset of fMLP superfusion.

The influence of the circulating concentration of FLMs on the rate of adhesion to the endothelium was explored, as shown in Fig. 3. Spontaneous (control) adhesion of FLMs reached asymptotic levels with time of infusion that were dependent on sphere concentration (Fig. 3*A*). The asymptotic level attained after initiation of superfusion with fMLP also increased with

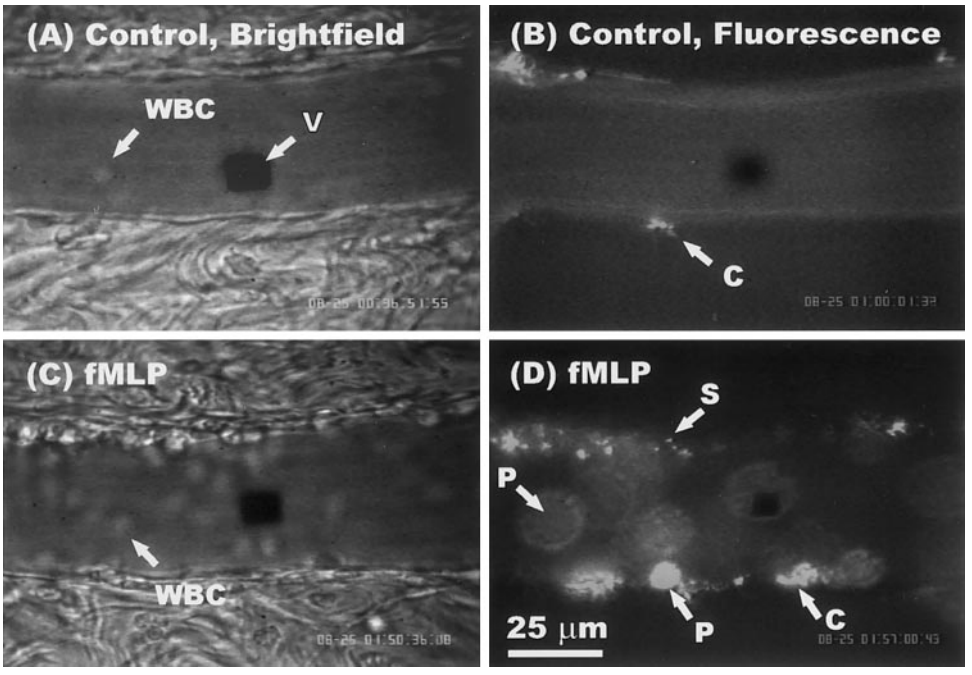

Fig. 1. Brightfield (*A*) and fluorescence (*B*) images of a postcapillary venule digitized before superfusion of the mesentery with 10^{-7} M *N*-formylmethionyl-leucyl-phenylalanine (fMLP). *C* and *D*: corresponding images of the same venule 42 min after initiation of fMLP superfusion. The number of fluorescently labeled microspheres (FLMs) increased from 12 (*B*) to 133 (*D*) per 100 μm of venule length. The number of leukocytes (WBCs) increased from 1 (*A*) to 20 (*C*) per 100 μm. V, image of the photodetector used to measure red blood cell velocity (V_{RBC}) during brightfield illumination; C, clusters of FLMs adhered to the endothelial cell (EC); P, point spread function of an out-of-focus sphere. Individual FLMs were best viewed when in focus (S in *D*).

sphere concentration (Fig. 3*B*). For both control and stimulated adhesion the time to reach maximal sphere accumulation was not strongly dependent on $[FLM]_{circ}$. Similarly, the stimulated increase in WBC adhesion was not significantly affected by the presence of all concentrations of FLMs (Fig. 3*C*). (The spontaneous adhesion of WBCs during control conditions was minimal because of a lack of tissue damage or a chemotactic agent and hence is not shown.)

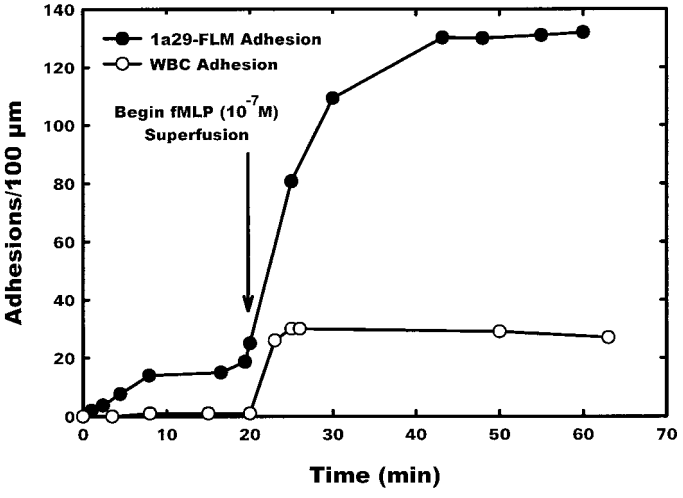

Fig. 2. Representative adhesion of 1a29-labeled fluorescent microspheres (1a29-FLM) and WBC per 100-μm venule length. At time t = 0, 1a29-FLMs were infused into the circulation via a femoral vein to achieve a circulating concentration of 4.23×10^6 spheres/mm^3. Adherent 1a29-FLM density reached a maximum within 20 min, at which time the tissue was superfused with Ringer solution containing 10^{-7} M fMLP. During the subsequent 40 min the adherent concentration of 1a29-FLMs and WBCs increased dramatically.

Maximum Adhesion

The maximum adhesion of 1a29-FLMs and WBCs asymptotically attained with time is summarized in Fig. 4 for control and fMLP conditions, where the abscissa refers to the circulating sphere concentration, $[FLM]_{circ}$. For the 1a29-FLMs, under control conditions (spontaneous adhesion) their accumulation increased almost linearly with $[FLM]_{circ}$ (Fig. 4*A*). However, maximal sphere adhesion rose asymptotically, reaching a maximum (150 per 100 μm) at ~8–11 $\times$ 10^6 spheres/mm^3. In contrast, the maximal levels of WBC adhesion, during either spontaneous (control) or stimulated (fMLP) adhesion, was invariant with $[FLM]_{circ}$ (Fig. 4*B*). A slight but insignificant decline in WBC adhesion was observed at a sphere concentration of 11×10^6/mm^3.

Rate of FLM Adhesion

The initial rate of adhesion of FLMs and WBCs for each $[FLM]_{circ}$ was determined by fitting the number of adhesion events with a first-order exponential of the form $N = A(1 - e^{-Bt})$, where N is the number of adhesions/100 μm at time t. Representative fits of these data are shown in Fig. 5, *A–C*, for $[FLM]_{circ}$ of 10.87×10^6/mm^3. The initial rate of adhesion (dN/dt) was calculated as the product $A \cdot B$ and is shown as a function of $[FLM]_{circ}$ in Fig. 5, *D–F*. The initial rate of spontaneous 1a29-FLM adhesion (Fig. 5*D*) was significantly dependent on $[FLM]_{circ}$, as determined by linear regression ($P < 0.026$), thus signifying the enhanced convective and diffusive transport of FLMs to the endothelium with increasing sphere concentration. The rates of fMLP-stimulated 1a29-FLM (Fig. 5*E*) adhesion were independent of $[FLM]_{circ}$ ($P = 0.215$), thus suggesting that FLM binding was affected more by the

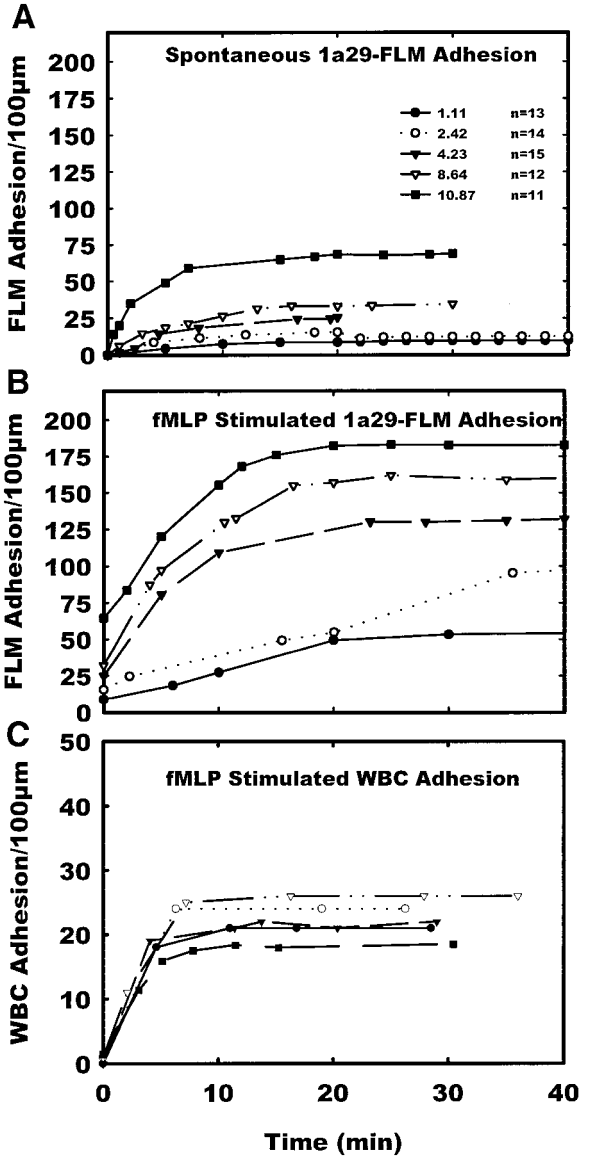

Fig. 3. Transient adhesion of FLMs under control conditions (*A*), FLMs after superfusion with 10^{-7} M fMLP (*B*), and WBCs after superfusion with fMLP (*C*). Shown are curves for the indicated circulating sphere concentrations (10^6/mm^3). Each curve is the average of n venules indicated. Standard deviations are omitted for clarity.

availability of ICAM-1 than by the availability of spheres. The invariance of the rate of fMLP-stimulated WBC adhesion with FLM concentration (Fig. 5*F*; $P = 0.727$) suggests that the presence of the spheres did not adversely affect WBC-EC adhesion by competing for binding sites.

Micropipette Infusion Experiments

To explore the basis for the more rapid accumulation of 1a29-FLMs compared with WBCs in response to fMLP stimulation, FLMs were infused directly into venules with micropipettes before and after removal of the glycocalyx with heparinase. The micropipettes were filled with concentrations similar in magnitude to those established by systemic infusion, i.e., $[FLM]_{circ}$ equal to 2.42, 8.46, and 10.87 $\times$ 10^6/mm^3. Comparison of the systemic and micropipette infusions at identical $[FLM]_{circ}$ yielded statistically similar rates of accumulation and levels of 1a29-FLM adhesion (data not shown). Two protocols were used for the micropipette experiments. The first protocol involved a control period (20 min), followed by fMLP superfusion (10^{-7} M, 20 min), and finally heparinase infusion (1 U/ml, 10 min) followed by a measurement period (20 min). The second protocol involved a control period (20 min) followed by a heparinase infusion (1 U/ml, 10 min) and then fMLP superfusion (10^{-7} M, 20 min). The infusion flow rate of the heparinase was matched to that of the cannulated vessel.

Average values of V_{RBC}, D, and wall shear rate for all periods of data acquisition (control and fMLP and heparinase protocols) are summarized in Table 1. No significant differences between hemodynamic parameters were apparent in the 85 venules studied.

Heparinase infusion followed by fMLP suffusion. Micropipette infusion of heparinase after a control period

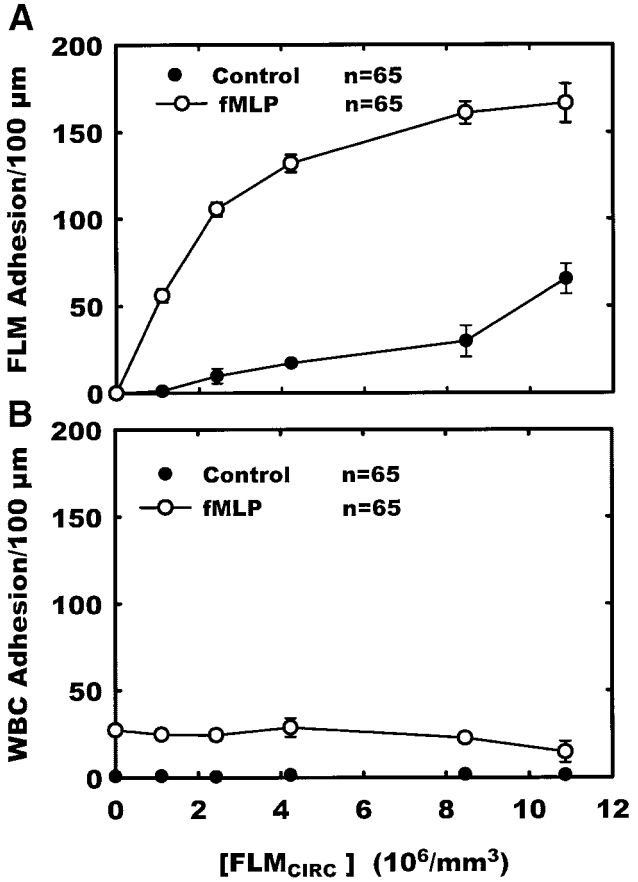

Fig. 4. *A*: maximum number of FLMs adhered per 100-µm venule length, under control conditions and after superfusion of the tissue with fMLP, as a function of the circulating concentration of FLMs ($[FLM]_{circ}$). The maximum adhesion was determined as the asymptotic value reached after 20 min, as depicted in Fig. 3. *B*: corresponding maximum amount of WBC adhesion per 100 µm vs. $[FLM]_{circ}$ during control and suffusion with fMLP (10^{-7} M). All data are shown as means ± SD for the indicated number of venules (n).

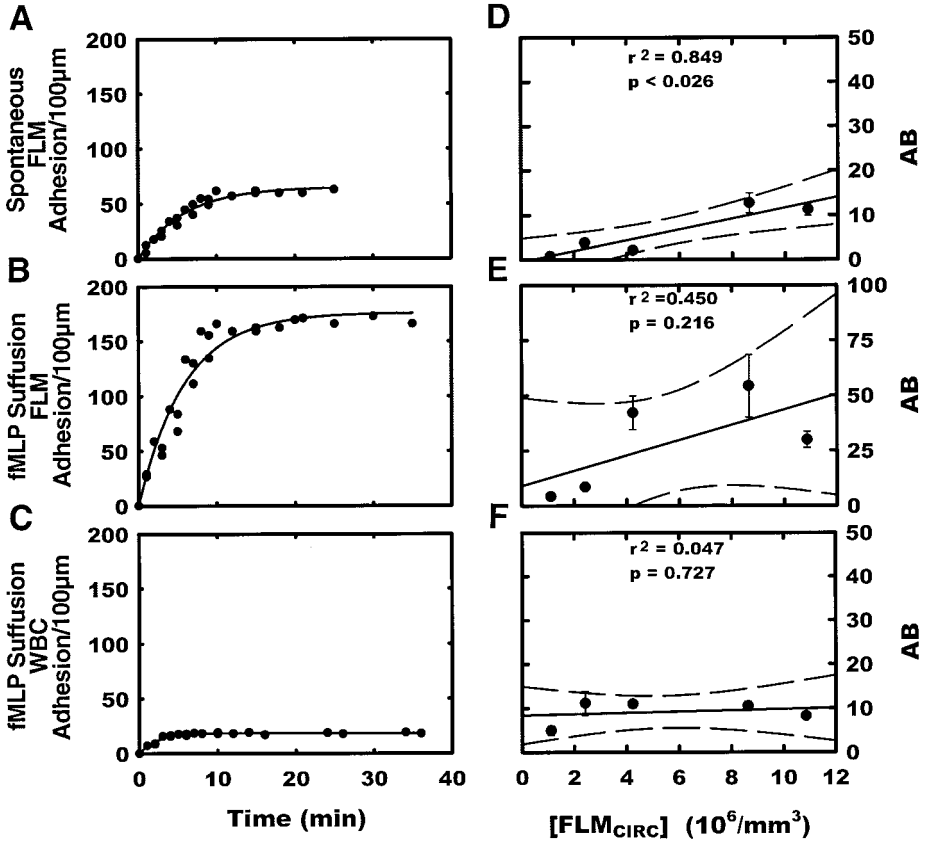

Fig. 5. Endothelial adhesion transients of FLMs during a control period of spontaneous adhesion (*A*), FLMs during a period of suffusion of the mesenteric tissue with Ringer solution containing 10^{-7} M fMLP (*B*), and WBCs during fMLP suffusion (*C*). All measurements were taken at $[FLM]_{circ} = 10.87 \times 10^6/mm^3$. Each set of trends was fit with a first-order exponential of the form $N = A(1 - e^{-Bt})$, where N is the number of adhesions/100 μm at time t. The corresponding initial particle accumulation rate, dN/dt, equals the product $A \cdot B$ and is shown in *D–F* as a function of $[FLM]_{circ}$. As indicated by the regression coefficients (r) in *D–F*, only the initial accumulation rate of FLMs during the control period varied significantly with sphere concentration ($P < 0.026$). The presence of the circulating FLMs did not affect the rate of WBC accumulation ($P = 0.727$). In all cases, an FLM concentration ranging from 8 to $11 \times 10^6/mm^3$ ensured the absence of concentration effects on adhesion.

of 1a29-FLM adhesion significantly increased 1a29-FLM adhesion ($P < 0.001$) to a maximum value that was independent ($P = 0.88$) of $[FLM]_{circ}$ (Fig. 6). The superfusion of fMLP 20 min after perfusion with heparinase did not cause a significant ($P = 0.94$) increase in FLM adhesion for any $[FLM]_{circ}$. Similarly, the maximum adhesion of the 1a29-FLMs after fMLP superfusion was independent of $[FLM]_{circ}$ ($P = 0.74$).

Table 1. *Hemodynamic parameters for postcapillary venules*

	Control	fMLP	Heparinase
Vessels first superfused with fMLP, then infused with heparinase			
No. of venules	70	81	70
Diameter, μm	39.5 ± 8.1	39.3 ± 10.3	36.7 ± 10.9
V_{RBC}, mm/s	2.68 ± 0.11	2.66 ± 0.50	2.42 ± 0.13
Shear rate, s^{-1}	512.6 ± 130.0	512.1 ± 166.8	497.1 ± 59.6
Vessels first infused with heparinase, then superfused with fMLP			
No. of venules	70	70	70
Diameter, μm	38.6 ± 12.1	39.2 ± 8.9	37.2 ± 10.2
V_{RBC}, mm/s	2.38 ± 0.25	2.53 ± 0.17	2.33 ± 0.34
Shear rate, s^{-1}	518.0 ± 177.8	495.8 ± 157.4	506.9 ± 139.6

Values are means ± SD of parameters measured in the micropipette perfusion protocols during the indicated treatment periods. FMLP, *N*-formylmethionyl-leucyl-phenylalanine; V_{RBC}, centerline red blood cell velocity. No significant differences were apparent among the 3 treatments.

The fraction of the free stream WBC flux that rolled along the venule wall, F_{WBC} (Fig. 7*A*), decreased significantly ($P < 0.03$) from control values after heparinase treatment. After fMLP superfusion was started, F_{WBC} remained unchanged. All changes in F_{WBC} were independent of $[FLM]_{circ}$. WBC firm adhesion (Fig. 7*B*) remained unchanged ($P = 0.48$) throughout the heparinase infusion and fMLP superfusion periods. The absence of significant changes in V_{RBC} (Fig. 7*C* and Table 1) suggests that alterations in flow or wall shear rate did not contribute to the results.

fMLP suffusion followed by heparinase infusion. Direct micropipette infusion of 1a29-FLM under control conditions followed by fMLP superfusion (Fig. 8) resulted in FLM adhesion levels similar to those attained by the systemic infusion technique (Fig. 4*A*). Maximal FLM adhesion 20 min after initiation of fMLP superfusion was dependent on $[FLM]_{circ}$ and increased from 100 to 150 spheres/100 μm as $[FLM]_{circ}$ was increased from 2.42 to $10.87 \times 10^6/mm^3$. The infusion of 1a29-FLM was temporarily stopped (by changing the pipette) while heparinase was infused. After heparinase infusion, the 1a29-FLM infusion was restarted and 1a29-FLM adhesion increased significantly ($P < 0.05$) to a similar maximum value of 180 spheres/100 μm for all $[FLM]_{circ}$, which was independent of $[FLM]_{circ}$ ($P = 0.89$).

As shown in Fig. 9*A*, fMLP superfusion after the control period resulted in a significant 50% decrease in

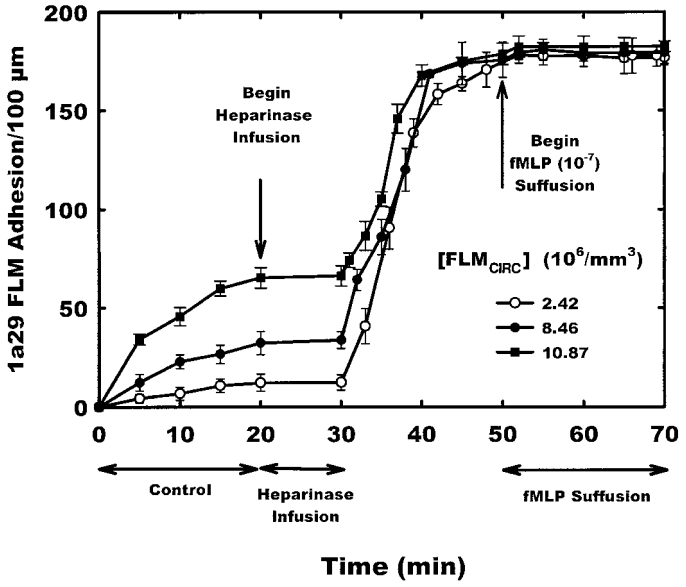

Fig. 6. Adhesion of FLMs during micropipette infusion, averaged for 15 venules for each of the indicated $[FLM]_{circ}$. After a 20-min control period, the infusion solution was changed to heparinase (1 U/ml), and the venules were perfused for 10 min at a rate of 4×10^{-4} mm^3/s. Infusion of FLMs was then resumed and continued for an additional 20 min, after which the tissue was suffused with 10^{-7} M fMLP. All data are shown as means ± SD.

F_{WBC} ($P < 0.03$), which was independent of $[FLM]_{circ}$ ($P = 0.74$). F_{WBC} remained significantly lower ($P = 0.045$) than control values after heparinase infusion and did not change significantly from the post-fMLP values. These trends were independent of $[FLM]_{circ}$. In contrast, firm adhesion of WBCs (Fig. 9*B*) increased significantly ($P < 0.001$) from control values after fMLP superfusion and was independent ($P = 0.96$) of $[FLM]_{circ}$. After heparinase infusion WBC adhesion decreased significantly ($P < 0.001$) from the post-fMLP values and was independent ($P = 0.82$) of $[FLM]_{circ}$. These results do not appear to be influenced by variations in V_{RBC} or wall shear rate, as evidenced by the insignificant variations in V_{RBC} and wall shear rate indicated in Fig. 9*C* and Table 1.

DISCUSSION

It is well established that topical application of chemotactic agents to exteriorized microvascular preparations results in a rapid accumulation of adherent WBCs in postcapillary venules. However, it is not clear how much of this response may be attributed to WBC or EC activation. For example, topical application of fMLP gives rise to a sevenfold increase in adhesion within 30 s, to increase adhesion from 1 to 7 WBCs per 100-µm length of postcapillary venules, and within 3 min as many as 12 WBCs adhere per 100 µm (11). This level of WBC-EC adhesion produces a twofold increase in the resistance to flow within postcapillary venules.

The rapid increase of 1a29-coated microspheres (FLMs) demonstrated in Fig. 2 in response to topically applied fMLP is suggestive of a dominant EC component. Given that the response time is much shorter than that required for protein synthesis and upregulation of ICAM-1 on the EC surface (7), it is plausible that constitutive levels of ICAM-1, although fairly low, may be shielded from forming adhesive contact with FLMs or WBCs. Visual inspection of the deposition of FLMs on the EC during stimulation reveals a patchy

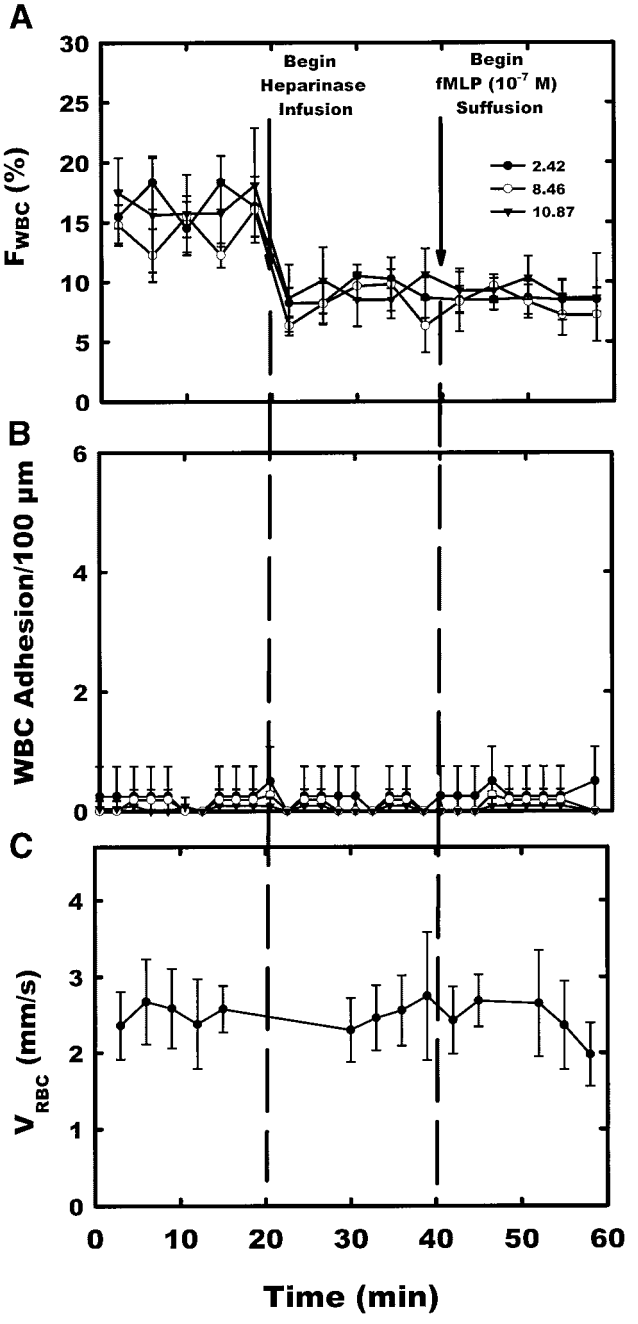

Fig. 7. Variations of the fractional flux of WBCs rolling along the venular wall (F_{WBC}; *A*), number of WBCs adhering per 100-µm venule length (*B*), and V_{RBC} (*C*) corresponding to the protocols described in Fig. 6 for micropipette perfusion of individual venules. The concentration of FLMs (10^6/mm^3) is shown as in Fig. 6. Periodic samplings of venular V_{RBC} reflect an absence of flow variations that could affect rolling and adhesion. Heparinase caused a significant drop in WBC rolling flux, which was not affected by the topical application of fMLP.

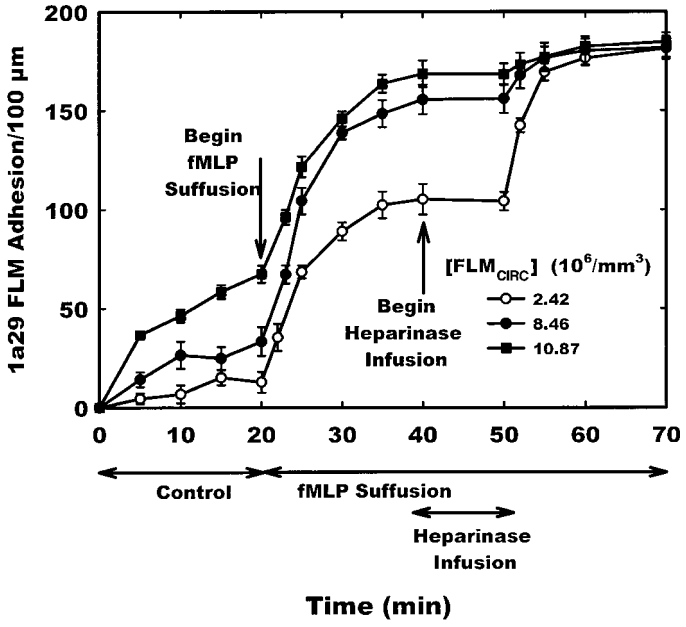

Fig. 8. Adhesion of FLMs during micropipette infusion, averaged for 15 venules for each of the indicated $[FLM]_{circ}$. The measurements were made as described in Fig. 6, except that the order of fMLP suffusion and heparinase infusion were reversed. Perfusion of the venules with heparinase significantly increased the number of FLMs adhering above the levels induced by fMLP.

distribution along the venular length, similar in sparseness to the adhesion of WBCs (Fig. 1). In contrast, studies of the distribution and binding of fluoresceinated 1a29 to the venular EC revealed a much more homogeneous deposition of MAb (13). With the use of confocal microscopy on fixed tissues, these studies suggest that although the constitutive expression of ICAM-1 was markedly heterogeneous throughout the hierarchy of arterioles, capillaries, and venules, within individual venules MAb binding to ICAM-1 was uniformly distributed over long sections of venules. Thus it appears that a barrier limits the binding of FLMs to the EC, and it is hypothesized here that the glycocalyx may shield ICAM-1 from binding by FLMs.

Evidence suggests that ICAM-1 may extend only 18.7 nm above the surface of the endothelium (25), whereas various constituents of the glycocalyx may consist of much larger and longer molecules. Most common macromolecular components of the glycocalyx are carbohydrates and glycoproteins such as glycosaminoglycans (GAGs) and glycolipids (20). The primary GAGs, heparan sulfate and chondroitin sulfate, are attached to large transmembrane proteins to form the proteoglycans (syndecans). The ICAM-1 molecule (76–114 kDa) is dwarfed in size compared with the syndecan core protein (~69 kDa) plus attached heparan sulfate GAGs (41.5 and 60 kDa). Typically, syndecans carry multiple heparan sulfate molecules and have a total mass ranging from 160 to 400 kDa (14), which, on the basis of molecular weight, overshadows ICAM-1.

In vitro attempts to measure the thickness of the glycocalyx have been dominated by histochemical methods that have revealed a range from 20 to 100 nm (19). The presence of a functionally larger layer thickness has been suggested by in vivo observations of the increase in capillary hematocrit after removal of the glycocalyx with heparinase (5). These studies suggest that the glycocalyx may extend on the order of 1 μm into the lumen. Observations in vivo with membrane-bound fluorescent dyes and fluorescently labeled dextrans in plasma (28) have suggested a functional thickness of the glycocalyx ranging from 400 to 500 nm. In

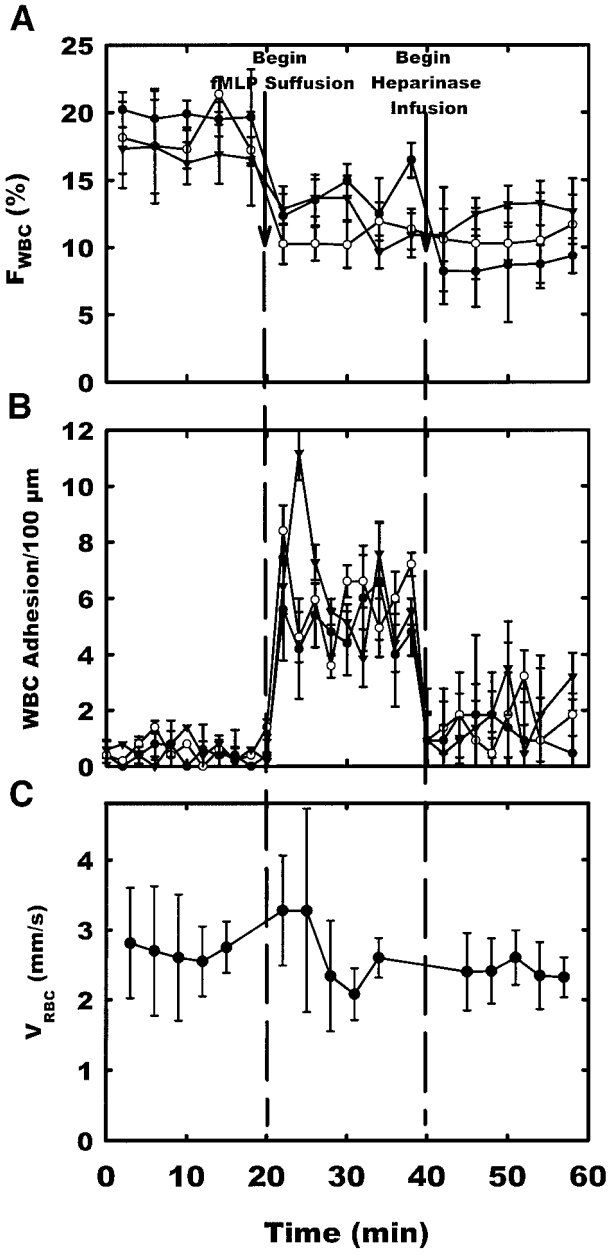

Fig. 9. Variation in the F_{WBC} (*A*), number of WBCs adhering per 100-μm venule length (*B*), and V_{RBC} (*C*) corresponding to the protocols described in Fig. 8 for micropipette perfusion of individual venules. The increase in WBC adhesion in response to fMLP is typical. The decrease in WBC adhesion with perfusion of heparinase reflects the effects of diminished selectin-mediated rolling that precludes WBC contact with the EC.

vivo studies of the permeation of the glycocalyx with anionic tracer molecules reveal a dependence of the penetration of the glycocalyx on molecular size, charge, and structure (29). Thus it is plausible that the presence of a 0.1-μm diameter polystyrene sphere attached to the 1a29 MAb limits its penetration into the glycocalyx and subsequent binding to ICAM-1.

The use of fluorescently coated microspheres in vivo has the additional advantage of permitting rapid visualization of an extremely small number of binding sites. The dense loading of each sphere with a large number of fluorophores renders their presence and position easily detectable within the focal plane and along the vertical optical axis without the necessity of resorting to confocal microscopy. The 0.1-μm-diameter spheres appear to be small enough that the hydrodynamic drag force that tends to remove each sphere from the endothelium is an order of magnitude below that of drag forces acting on particles the size of a leukocyte (23). The density of labeling of MAb on the surface of the sphere used here (88 1a29 molecules/sphere) amounts to ~2,800 1a29 molecules/μm^2. This is far greater than estimates of the surface density of adhesive bonds derived from in vivo measurements of the adhesive force between WBCs and ECs in postcapillary venules (12). As shown in that study, the contact zone between WBCs and ECs may possess on the order of 30 bonds per WBC, and on the basis of the typical contact areas between the two cells a bond density on the order of 2 bonds/μm^2 may be present. Thus the adhesion of 1a29-coated FLMs to the EC does not appear to be dependent on prevailing levels of wall shear stresses and reflects mainly the availability of ICAM-1 binding sites. Flow-dependent effects were generally precluded by the maintenance of similar levels of wall shear rate for all treatments (Table 1).

The baseline level of FLM adhesion before application of fMLP (Fig. 2) or infusion of heparinase (Fig. 6) appears to be a nonlinear function of the concentration of circulating spheres (Fig. 4*A*) as well as the availability of ICAM-1 binding sites. In general, the accumulation of FLMs on the EC surface will depend on the equilibrium between convection of spheres to potential binding sites, the kinetics of bond formation and disruption, and the levels of hydrodynamic forces tending to remove the FLMs from the EC. In light of the trends in Fig. 4*A*, it appears that for sphere concentrations of 8 and 11 $\times$ 10^6/mm^3 the convection of spheres to the EC does not affect the results.

The longer time to achieve an asymptotic value for lesser FLM concentrations (Fig. 3*A*) may also reflect the rate of sphere uptake by other sites during systemic infusion. It has been shown that large regional differences in constitutive and induced ICAM-1 expression vary widely among organs (17). For example, as shown in that study, splanchnic beds have a constitutive level of ICAM-1 that is 1/50th of that of the lung. Comparison of the present baseline level of sphere adhesion (≈50 spheres/100 μm; Fig. 4*A*) with similar measures of ICAM-1 expression in lung (7) reveals disparities that may reflect organ-specific and topographical differences within a given network. In that study, by studying the accumulation of avidin-labeled microspheres (0.28-μm diameter) to biotin-labeled MAb to ICAM-1, a constitutive level of two spheres per 175,000 μm^2 was found. Normalization of these values to the surface area of a typical 100-μm-long venular section in the present study (10,000 μm^2) yields an equivalent level of binding equal to 0.02 spheres/100 μm, which is 1/2,500th of the baseline level observed here. This disparity may reflect differences in sensitivity of the methods employed, the substantially greater density of ICAM-1 in the small postcapillary venules of the mesentery, and/or the greater exclusion of the larger microspheres by the glycocalyx.

Studies of the upregulation of ICAM-1 in pulmonary microvessels (7) reveal a 1- to 4-h time after TNF-α challenge to produce a threefold upregulation of ICAM-1, with one-third of its maximal expression occurring at 1 h and peak expression at 4 h after stimulation. Thus the threefold increase in FLM adhesion observed in the present study after 20 min of fMLP stimulation (Fig. 8) suggests that ICAM-1 rapidly becomes more accessible to FLMs or WBCs after exposure to fMLP.

It is conceivable that the enhanced accessibility of ICAM-1 results from shedding of the glycocalyx after EC activation. To explore this hypothesis, FLM and WBC adhesion were examined before and after perfusion of individual venules with heparinase. It is evident that maximal FLM adhesion was attained after removal of the glycocalyx with heparinase and that subsequent stimulation with fMLP did not result in an incremental increase (Fig. 6). The results shown in Fig. 8 for FLMs suggest that fMLP adhesion alone did not saturate all potential binding sites on the EC for FLMs, because subsequent infusion of heparinase produced an additional increment of FLM adhesion. In both protocols, the rolling flux of WBCs was on the order of 40% after the control period.

The decline in F_{WBC} after fMLP superfusion (Fig. 9*B*) has been observed previously (12) and may reflect WBC depletion of the rolling stream as WBCs accumulate along the EC with the stimulated adhesion. The number of adhered WBCs at any instant of time represents a balance of WBC adhesion and removal rates. The fall in WBC adhesion after heparinase treatment (Fig. 9*B*) and the decreased flux in response to heparinase alone (Fig. 7*A*) most likely reflect a diminished ability to support selectin-mediated rolling resulting from removal of the glycocalyx and associated E- or P-selectins. Because WBCs cannot roll along the EC, adhesion cannot be enhanced with fMLP (Fig. 7*B*). Hence, it is thus possible that fMLP activation of the EC results in a shedding of the glycocalyx that is comparable to its removal with heparinase. This behavior is consistent with in vitro observations that heparinase inhibited 80% of L-selectin-mediated monocyte attachment to TNF-α-activated aortic endothelium (9). Similarly, it has been shown that P-selectin must extend a minimum distance from the plasma membrane to support WBC rolling (18).

It is thus evident from the present studies that the glycocalyx presents a physical barrier between WBCs and ECs that may play an important role in mediating the inflammatory response. As a means of elucidating its role, the present study represents a first step that may lead to other more direct biochemical analyses of molecular alterations in the glycocalyx with EC activation. It should be noted that the precise mechanism by which fMLP acts directly to activate the endothelium or promote exposure of ICAM-1 on its surface warrants further study. It is conceivable that fMLP activation of other cells in the tissue, e.g., mast cells, may play a role. However, because the initial adhesion response is so rapid and the spatial distribution of mast cells in mesentery low and distant from the EC, this pathway is unlikely.

The authors express their appreciation to Karen Trippett for technical assistance and Dr. Donald Anderson, Pharmacia-Upjohn, for providing copious amounts of 1a29.

This work was supported by National Heart, Lung, and Blood Institute Grant HL-39286.

REFERENCES

1. **Akerstrom B, Brodin T, Reis K, and Bjorck L.** Protein G: a powerful tool for binding and detection of monoclonal and polyclonal antibodies. *J Immunol* 135: 2589–2592, 1985.
2. **Arfors KE, Lundberg C, Lindbom L, Lundberg K, Beatty PG, and Harlan JM.** A monoclonal antibody to the membrane glycoprotein complex CD18 inhibits polymorphonuclear leukocyte accumulation and plasma leakage in vivo. *Blood* 69: 338–340, 1987.
3. **Atherton A and Born GVR.** Quantitative investigation of the adhesiveness of circulating polymorphonuclear leukocytes to blood vessel walls. *J Physiol* 222: 447–474, 1972.
4. **Bjork J, Lindbom L, Gerdin B, Smedegard G, Arfors KE, and Benveniste J.** Paf-acether (platelet-activating factor) increases microvascular permeability and affects endothelium-granulocyte interaction in microvascular beds. *Acta Physiol Scand* 119: 305–308, 1983.
5. **Dejardins C and Duling BR.** Heparinase treatment suggests a role for the endothelial cell glycocalyx in the regulation of capillary hematocrit. *Am J Physiol Heart Circ Physiol* 258: H647–H654, 1990.
6. **Fernandez-Lafuente R, Rosell CM, Rodriguez V, Santana C, Soler G, Bastida A, and Guisan JM.** Preparation of activated supports containing low pK amino groups. A new tool for protein immobilization via the carboxyl coupling method. *Enzyme Microb Technol* 15: 546–550, 1993.
7. **Fingar VH, Taber SW, Buschemeyer WC, Ten Tije A, Cerrito PB, Tseng M, Guo H, Johnston MN, and Wieman TJ.** Constitutive and stimulated expression of ICAM-1 protein on pulmonary endothelial cells in vivo. *Microvasc Res* 54: 135–144, 1997.
8. **Firrell JC and Lipowsky HH.** Leukocyte margination and deformation in mesenteric venules of rat. *Am J Physiol Heart Circ Physiol* 256: H1667–H1674, 1989.
9. **Giuffre L, Cordey AS, Monai N, Tardy Y, Schapira M, and Spertini O.** Monocyte adhesion to activated aortic endothelium: role of L-selectin and haparan sulfate proteoglycans. *J Cell Biol* 136: 945–956, 2000.
10. **Harlan JM.** Leukocyte-endothelial interactions. *Blood* 65: 513–525, 1985.
11. **House SD and Lipowsky HH.** Leukocyte-endothelium adhesion: microhemodynamics in mesentery of the cat. *Microvasc Res* 34: 363–379, 1987.
12. **House SD and Lipowsky HH.** In vivo determination of the force of leukocyte to endothelium adhesion in the mesenteric microvasculature of the cat. *Circ Res* 63: 658–668, 1988.
13. **Iigo Y, Suematsu M, Higashida T, Oheda J, Matsumoto K, Wakabayashi Y, Ishimura Y, Miyasaka M, and Takashi T.** Constitutive expression of ICAM-1 in rat microvascular systems analyzed by laser confocal microscopy. *Am J Physiol Heart Circ Physiol* 273: H138–H147, 1997.
14. **Kato M, Wang H, Bernfield M, Gallagher JT, and Turnbull JE.** Cell surface syndecan-1 on distinct cell types differs in fine structure and ligand binding of its heparan sulfate chains. *J Biol Chem* 269: 18881–18890, 1994.
15. **Ley K, Bullard DC, Arbones ML, Bosse R, Vestweber D, Tedder TF, and Beaudet AL.** Sequential contribution of L- and P-selectin to leukocyte rolling in vivo. *J Exp Med* 181: 669–675, 1995.
16. **Lipowsky HH and Zweifach BW.** Application of the two-slit photometric technique to the measurement of microvascular volumetric flow rates. *Microvasc Res* 15: 93–101, 1978.
17. **Panes J, Perry MA, Anderson DC, Manning A, Leone B, Cepinskas G, Rosenbloom CL, Miyasaka M, Kvietys PR, and Granger DN.** Regional differences in constitutive and induced ICAM-1 expression in vivo. *Am J Physiol Heart Circ Physiol* 269: H1955–H1964, 1995.
18. **Patel KD, Nollert MU, and McEver RP.** P-selectin must extend a sufficient length from the plasma membrane to mediate rolling of neutrophils. *J Cell Biol* 131: 1893–1902, 1995.
19. **Pries AT, Secomb TW, and Gaehtgens P.** The endothelial surface layer. *Pflügers Arch* 440: 653–666, 2000.
20. **Rambourg A and Leblond CP.** Electron microscope observations on the carbohydrate-rich cell coat present at the surface of cells in the rat. *J Cell Biol* 32: 27–53, 1967.
21. **Schmid-Schönbein GW, Skalak R, Simon SI, and Engler RL.** The interaction between leukocytes and endothelium in vivo. *Ann NY Acad Sci* 516: 348–361, 1987.
22. **Shinde Patil VR, Campbell CJ, Yun YH, Slack SM, and Goetz DJ.** Particle diameter influences adhesion under flow. *Biophys J* 80: 1733–1743, 2001.
23. **Springer TA.** Adhesion receptors of the immune system. *Nature* 346: 425–434, 1990.
24. **Staunton DE, Dustin ML, Erickson HP, and Springer TA.** The arrangement of the immunoglobulin-like domains of ICAM-1 and the binding sites for LFA-1 and rhinovirus. *Cell* 61: 243–254, 1990.
25. **Tamatani T and Miyasaka M.** Identification of monoclonal antibodies reactive with the rat homolog of ICAM-1 and evidence for a differential involvement of ICAM-1 in the adherence of resting versus activated lymphocytes to high endothelial cells. *Int Immunol* 2: 165–171, 1990.
26. **Tompkins WR, Monti R, and Intaglietta M.** Velocity measurements by self-tracking correlator. *Rev Sci Instrum* 45: 647–649, 1974.
27. **Vejlens G.** The distribution of leukocytes in the vascular system. *Acta Pathol Microbiol Scand* 33: 159–190, 1938.
28. **Vink H and Duling BR.** Identification of distinct luminal domains for macromolecules, erythrocytes, and leukocytes within mammalian capillaries. *Circ Res* 79: 581–589, 1996.
29. **Vink H and Duling BR.** Capillary endothelial surface layer selectively reduces plasma solute distribution volume. *Am J Physiol Heart Circ Physiol* 278: H285–H289, 2000.
30. **Wayland H and Johnson PC.** Erythrocyte velocity measurements in microvessels by a two-slit photometric method. *Am J Physiol* 22: 333–337, 1967.